4 $^1P_1$ Zn excitation by 80-eV electrons

Mariusz Piwiński,* Łukasz Kłosowski, Dariusz Dziczek, and Stanisław Chwirot
Institute of Physics, Faculty of Physics, Astronomy and Informatics, Nicolaus Copernicus University in Toruń, Grudziądzka 5, 87-100 Toruń, Poland

Dmitry V. Fursa and Igor Bray
Curtin Institute for Computation and Department of Physics and Astronomy, Curtin University, GPO Box U1987, Perth WA 6845, Australia
(Received 16 March 2015; published 5 June 2015)

The electron-photon coincidence method in the coherence analysis version has been applied to characterize electron impact excitation of 4 $^1P_1$ state of zinc atoms for 80 eV. The experimental values of the Stokes parameters and the electron impact coherence parameters are presented together with convergent close coupling theoretical data. Our results are compared with recently published relativistic distorted-wave approximation calculations.

DOI: 10.1103/PhysRevA.91.062704 PACS number(s): 34.80.Dp, 34.80.Pa

I. INTRODUCTION

The electron impact excitation of atoms is one of the fundamental processes and has been widely and in depth studied since Franck and Hertz published their pioneering work [1]. In most cases, data obtained experimentally such as scattering cross sections, excitation, and polarization functions do not ensure full information on the process investigated. However, as suggested by Bederson [2] complete or nearly complete information on the electron impact excitation can be obtained using the electron-photon coincidence technique. Such data are very important for verification and refinement of theoretical models and lead to much better understanding of the impact excitation phenomena [3–12].

This is of special relevance to studies of electron collisions with zinc atoms due to a serious discrepancy between theory and experiment for the linear polarization Stokes parameter P_2 associated with spin-polarized electron-impact excitation of the $(3d^{10}4s5s)\ ^3S_1$ state from the ground state. The measurements of Pravica *et al.* [13] showed significantly nonzero polarization of the light due to the optical decay from the $(3d^{10}4s5s)\ ^3S_1$ state to the $(3d^{10}4s4p)\ ^3P_{0,1,2}$ states; however, all theoretical methods applied to this problem predict negligible polarization. Although the analysis of the situation [14] has led to some controversy [15,16], the discrepancy is still unresolved. It is important, therefore, to build up a body of knowledge relevant to electron impact on zinc with the aim of testing various aspects of the existing theoretical methods.

There has been a growing interest in studies of impact excitation of Zn atoms due to possible application in discharge lamps and a need for modeling of Zn plasma systems [17]. However, due to experimental difficulties the experimental data for Zn are still sparse, especially for large scattering angles and lower impact energies [18,19]. The former limitation can be overcome using the magnetic angle changer (MAC) technique [20] to access, besides the backscattering, the range of the forward scattering angles, but the main problem associated with long measurement time cannot be solved in a straightforward way. The superelastic scattering experiments might deliver as precise data as the coincidence studies in a much shorter time [21,22], but such an approach does not seem feasible in the case of Zn atoms because of problems and costs related to UV laser sources (213.9 nm) and lack of efficient polarizing optics for such a spectral band. Thus, the electron-photon coincidence technique seems the only approach allowing for quantum mechanically complete studies of the excitation process of interest.

The present study was also stimulated by the recent work of Das *et al.* [12], who carried out RDWA calculations for electron impact excitation of Zn atoms. Moreover, new data for excitation of Zn atoms at several impact energies complement the existing body of data for Ca and Zn and thus may allow comparative study proposed by Hamdy *et al.* [8]. Both elements have a very similar electron structure ([Ar]$4s^2$ and [Ar]$3d^{10}4s^2$, respectively) with a closed outer ns^2 shell. Hence, a comparison of the data for Zn and Ca may shed light on the contribution of the closed $3d^{10}$ shell in the scattering process leading to the excitation of the $4s^2$ shell to the $^1P_1$ state.

This work is a continuation of our study on electron-zinc atom collisions [18,19], which is a part of our broader research on He-like atoms: calcium [23,24], cadmium [25–27], and helium [28]. We present the set of experimental values of Stokes and electron impact coherence parameters (EICPs) for 80-eV incident electron energy, together with convergent close coupling (CCC) theoretical predictions. Our results are compared with the recently published results of RDWA modeling of the same excitation process [12].

II. APPARATUS AND EXPERIMENTAL PROCEDURE

The geometry of the experiment was typical for electron-photon coincidence measurements in the coherence analysis version. The apparatus and the procedure were the same as in our previous study [18]. A schematic diagram of the experimental setup is shown in Fig. 1.

Zinc target atoms were produced by the oven, which provided an atomic beam with number density of the order of 10^{10} cm^{-3} in the collision region. The electron beam of energy 80 eV with current of order 1 μA was produced by a commercial electron gun. Both beams were cross-fired in the collision region (diameter 1.5–2 mm) located 22 mm above the exit aperture of the two-stage collimator mounted on top of the

*mariusz.piwinski@fizyka.umk.pl

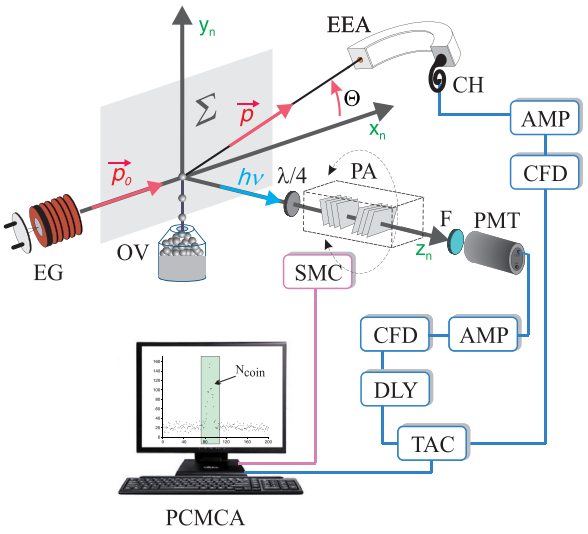

FIG. 1. (Color online) The schematic outline of the apparatus and geometry of the electron-photon coincidence experiment in the coherence analysis version. EG – electron gun, EEA – electron energy analyser, CH – channel electron multiplier, OV – the source of the atomic beam (stainless steel oven with two-stage collimator), $\lambda/4$ – zero-order quartz retardation plate, PA – pile-of-plates polarization analyzer, F – 213.9 nm filter, PMT – photomultiplier tube, CFD – constant fraction discriminator, SMC – stepper motor controller, TAC – time-to-amplitude converter, AMP – preamplifier, DLY – delay line, PCMCA – personal computer with multichannel analyzer. The scattering plane Σ is defined by $\mathbf{p_0}$ and $\mathbf{p}$, which are the momentum vectors of electron before and after the collision, respectively. Θ – the scattering angle.

oven. Zinc atoms excited to the 4 $^1P_1$ state were investigated by coincidence detection of energy-selected electrons, and photons emitted upon spontaneous decay to the ground state. The fluorescence photons (213.9 nm) were analyzed using polarization analyser system and detected in the direction perpendicular to the scattering plane. The scattered electrons were energy selected for 5.8 eV energy loss (corresponding to the studied excitation process) using an electron energy analyzer (EEA) fixed at the scattering angle Θ and detected with a channel electron multiplier. The electron pulses were used as start and the photon pulses as stop signals in the standard delayed coincidence circuit.

The true coincidence counts were determined in the usual way from the coincidence spectra by subtracting the background of false coincidences from the total number of counts integrated within the coincidence window. These values enabled determination of P_1 and P_2 Stokes parameters calculated according to formulas

$$P_1 = \frac{N_0 - N_{90}}{N_0 + N_{90}}, \quad P_2 = \frac{N_{45} - N_{-45}}{N_{45} + N_{-45}}, \tag{1}$$

where N_0, N_{90}, N_{45}, N_{-45} are numbers of true coincidence counts determined at four positions of polarization analyzer transmission axis. The circular polarization measurements were carried out with the $\lambda/4$ retardation plate. In this case the P_3 Stokes parameter was obtained from the equation

$$P_3 = \frac{N_{45C} - N_{-45C}}{N_{45C} + N_{-45C}}. \tag{2}$$

N_{45C} and N_{-45C} represent the values of true coincidence counts determined from coincidence spectra collected at the two relative positions of the linear polarizer and the $\lambda/4$ plate.

The experimental procedure involved repeated cycles of 300-s coincidence spectra accumulation at different positions of the polarizer to minimize the effects of possible long-term drifts of the experimental conditions. Stokes parameters (P_1, P_2, and P_3) for each scattering angle were determined in separate runs.

Total integration times varied with scattering angle and were of the order of 3 days for 10° to 3 weeks for 40°. The EICPs describing excitation process were determined from experimentally obtained values of Stokes parameters using the following formulas [4].

The shape of the electron charge cloud after the excitation is represented by P_{L} according to

$$P_{\mathrm{L}} = \sqrt{P_1^2 + P_2^2}. \tag{3}$$

The γ parameter describes the charge cloud alignment angle determined with respect to the direction of the incoming electron

$$\gamma = \tfrac{1}{2} \arg(P_1 + \mathrm{i}P_2), \tag{4}$$

and parameter $L_\perp$, the angular momentum transfer

$$L_\perp = -P_3. \tag{5}$$

The P^+ parameter characterizes the degree of coherence of the excitation process (in a full coherent case $P^+ = 1$):

$$P^+ = \sqrt{P_1^2 + P_2^2 + P_3^2}. \tag{6}$$

The parameters P_L and γ determine the angular distribution of the electron charge cloud of the excited atom given by

$$|\Psi(\vartheta,\phi)|^2 = \frac{3}{8\pi} \sin^2\vartheta [1 + P_L \cos 2(\phi - \gamma)], \tag{7}$$

where ϑ and ϕ are standard spherical coordinates.

III. CCC METHOD

We have used the CCC method to produce theoretical predictions for Stokes parameters and EICPs. The CCC method and its application to e-Zn scattering has been described in Ref. [29]. Here we present only a brief outline. The Zn atom is described by a model of two active electrons above an inert Hartree-Fock core. The inert-core orbitals are obtained by performing self-consistent Hartree-Fock calculations for the Zn^+ ion. The active orbitals are obtained by diagonalization of the Zn^+ Hamiltonian in the (Laguerre) Sturmian basis comprising $l = 0,1,2,3$ orbitals. The number (N_l) of active orbitals is chosen to be $N_0 = 9$, $N_1 = N_2 = 8$, $N_3 = 5$. These orbitals are used to form a set of antisymmetric two-electron configurations. All possible configurations where one of active electrons occupies $4s$ or $4p$ orbitals were formed and used to diagonalize the Zn Hamiltonian. The total number of target states is 206, comprising singlet and triplet states with

the orbital angular momentum up to four. We have used one- and two-electron polarization potentials to improve the accuracy of the Zn target states. The scattering calculations for e-Zn scattering are conducted by performing a multichannel expansion of the total wave function and formulating a system of coupled Lippmann-Schwinger equations for the T matrix. These equations are solved in a standard way [30], and scattering amplitudes, cross sections, and Stokes parameters are obtained for the transitions of interest. Finally, we note that for Zn a nonrelativistic formulation proves to be sufficient. This has been verified by performing calculations in a fully relativistic formulation of the CCC method [31] that produced results in close agreement with the present nonrelativistic approach.

IV. RESULTS AND DISCUSSION

We present the Stokes (Fig. 2) and EICPs (Fig. 3) for the electron energy of 80 eV. The experimental data obtained for the scattering angles in the range 10° to 40° are presented together with CCC theoretical predictions for the full range of scattering angles. The numerical values of experimentally determined Stokes parameters and EICP's are presented in Table I.

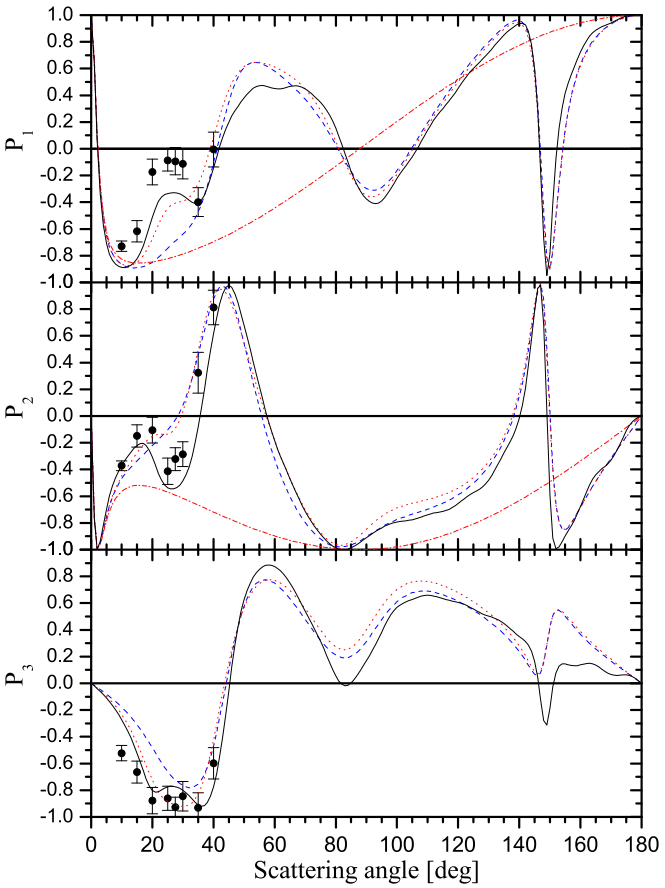

FIG. 2. (Color online) Stokes parameters (P_1, P_2, P_3) for electronic excitation (80 eV) of 4 $^1P_1$ Zn state. Experimental data (•) are presented together with (—) CCC, (– –) SC RDWA, and (· · ·) MC RDWA theoretical predictions [12]. In the case of P_1 and P_2 the results of FBA results (— · —) are also shown.

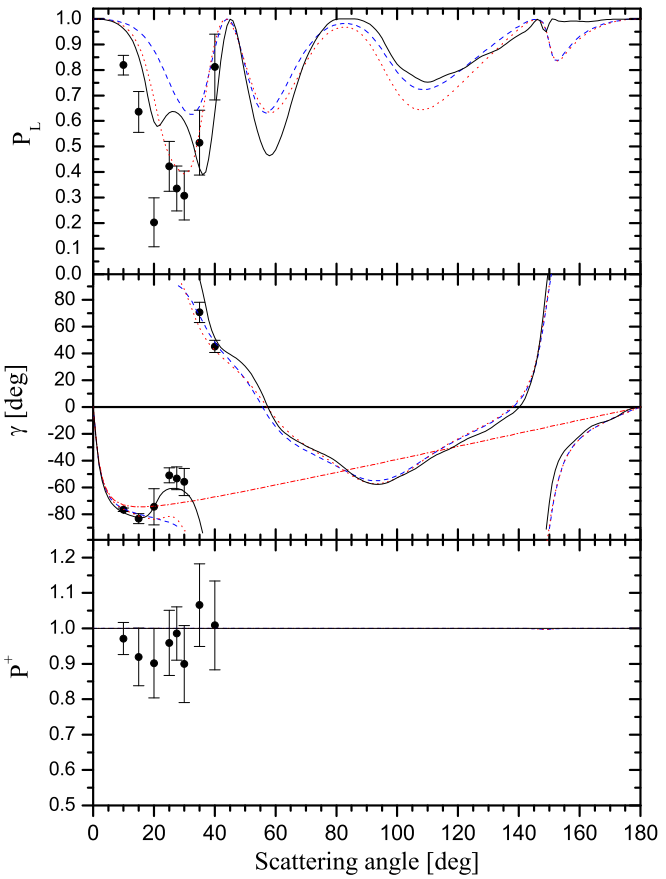

FIG. 3. (Color online) EICP parameters (P_L, γ, P^+) for electronic excitation (80 eV) of 4 $^1P_1$ Zn state. Experimental data (•) are presented together with (—) CCC, (– –) SC RDWA, and (· · ·) MC RDWA theoretical predictions [12]. In the case of γ the results of FBA results (— · —) are also shown.

Our data are compared with theoretical results obtained using the fully relativistic distorted wave approximation (RDWA) method for both single-configuration (SC RDWA) and multiconfiguration (MC RDWA) Dirac-Fock wave functions [12]. In addition, the first Born approximation (FBA) [4] values of the γ, P_1, and P_2 parameters are also presented.

The comparison of the Stokes parameters obtained experimentally and calculated using CCC, RDWA, and FBA models is presented in Fig. 2. Our experimental data are generally in good qualitative agreement with the CCC results. All the characteristic features of the angular dependence of the measured parameters are qualitatively reproduced by the CCC calculations, although there are some minor discrepancies between the measured and theoretical values. More significant differences occur for the RDWA calculations (both SC and MC) and FBA data.

Figure 3 presents comparison of the theoretical and experimental EICP values. At the scattering angles below 40°, both the CCC and experimental values of P_L parameter show similar structures (two local minima and one local maximum), which are not present in MC RDWA and SC RDWA predictions. The experimental values of the γ parameter show local maximum at 25° scattering angle, clearly visible in CCC predictions, slightly noticeable in MC RDWA results,

TABLE I. Stokes parameters and EICPs for excitation of Zn atoms to the 4 $^1P_1$ state by 80 eV electrons. Listed experimental uncertainties are single standard deviations.

Θ(deg)	P_1	P_2	$P_3 = -L_\perp$	P_L	γ(deg)	P^+
10	−0.73 ± 0.04	−0.37 ± 0.04	−0.52 ± 0.06	0.82 ± 0.04	−77 ± 2	0.97 ± 0.05
15	−0.62 ± 0.08	−0.15 ± 0.09	−0.66 ± 0.09	0.64 ± 0.08	−83 ± 4	0.92 ± 0.09
20	−0.17 ± 0.10	−0.11 ± 0.10	−0.88 ± 0.10	0.20 ± 0.10	−74 ± 14	0.90 ± 0.10
25	−0.09 ± 0.09	−0.41 ± 0.10	−0.86 ± 0.10	0.42 ± 0.10	−51 ± 6	0.96 ± 0.10
27.5	−0.09 ± 0.10	−0.32 ± 0.09	−0.93 ± 0.08	0.34 ± 0.09	−53 ± 9	0.99 ± 0.08
30	−0.11 ± 0.12	−0.29 ± 0.10	−0.85 ± 0.11	0.31 ± 0.10	−56 ± 11	0.90 ± 0.11
35	−0.40 ± 0.11	0.32 ± 0.15	−0.93 ± 0.12	0.51 ± 0.13	+71 ± 8	1.07 ± 0.12
40	−0.01 ± 0.13	0.81 ± 0.13	−0.60 ± 0.12	0.81 ± 0.13	+45 ± 5	1.01 ± 0.13

and unobserved in SC RDWA data. According to the FBA assumptions the P_L parameter has a value of one and the γ curve shows only one minimum.

In the case of P_1 the experimental data have lower values than the theoretical ones, which is also reflected in the graph of P_L parameter. However, the experimentally obtained coherence parameter P^+ has a value of 1 (within the limits of measurements uncertainty), which confirms the fully coherent scattering process assumption (Percival Seaton hypothesis [32]). These results indicate that measured parameters were not significantly affected by systematic errors such as radiation trapping causing partial depolarization of the detected fluorescence.

The variation between different theoretical and experimental sets of the EICPs is illustrated in Fig. 4 for the scattering angle of 30°.

An alternative way of presenting both P_L and γ parameters in a concise form is drawing P_1 and P_2 on a polar plot as a function of the scattering angle [4], where

$$P_1 + iP_2 = P_L \exp(2i\gamma). \tag{8}$$

P_L represents the length of the polarization vector defined by P_1 and P_2, and 2γ is the angle between P_1 axis and its direction.

Figure 5 presents a comparison of all the results for the P_1 and P_2 in the range of 10° to 45°. For symmetry reasons $P_2 = P_3 = 0$ at scattering angle $\Theta = 0°$. Therefore all the curves start at $(P_1, P_2) = (1,0)$ and end at the same point. Starting from the (1,0) point and going along one of the curves in the clockwise direction one can analyze the relations between the P_1 and P_2 for different scattering angles.

The FBA data are located on the unit circle, starting and ending at point (1,0) (Fig. 5). The straight lines visible in the first part of the CCC and RDWA curves are associated with the resolution of calculations (1°) and very rapid changes of P_1 and P_2 parameter values in the range of low scattering angle. Starting from the (1,0) point, which is equivalent to $\Theta = 0°$, one can see that all the theoretical data are in almost perfect agreement until P_1 reaches the value of −0.86 corresponding to $\Theta = 16°$. From this point the FBA curve is going back to the (1,0) point on the same path. The other theoretical

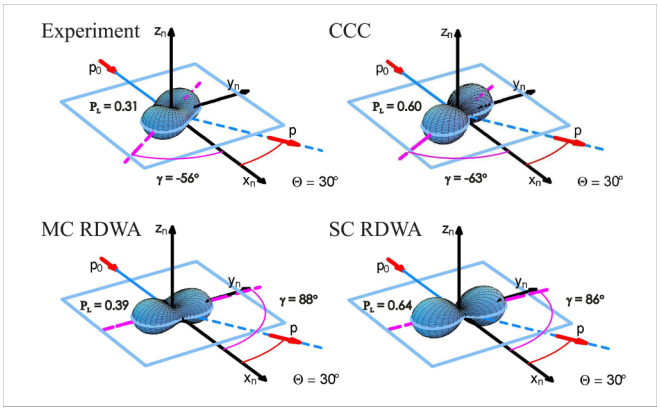

FIG. 4. (Color online) Graphical representations of angular distributions of the electron charge cloud of the excited 4 $^1P_1$ state of Zn for experimentally and theoretically obtained values of the EICPs at 30° scattering angle.

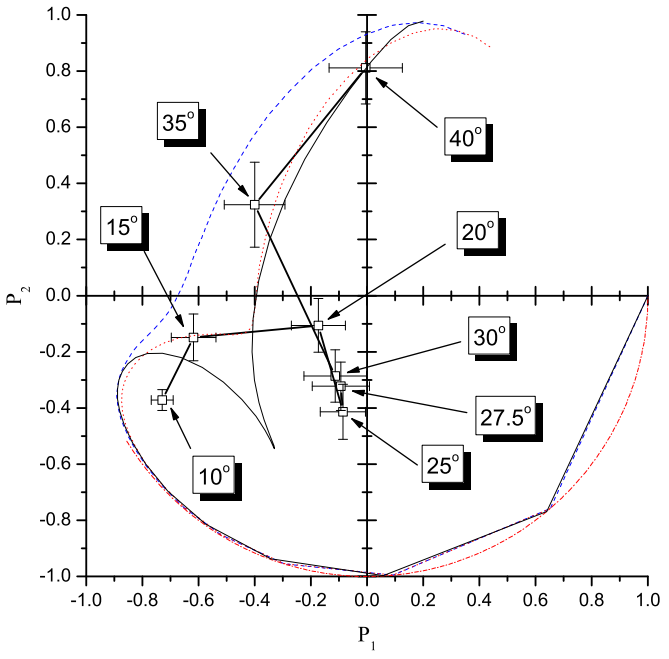

FIG. 5. (Color online) Polar plot of $P_1 + iP_2$ for electronic excitation (80 eV) of 4 $^1P_1$ Zn state in the range of 10° to 45°. Experimental data (□) with the straight line to guide the eye, (—) CCC, (– –) SC RDWA, and (· · ·) MC RDWA. The FBA theoretical predictions (— · —) are located on the unit circle; see explanation in the text. Experimental data are shown together with corresponding values of the scattering angles.

curves spread in different directions and finally meet again at point (0.34,0.94) corresponding to $\Theta = 45^\circ$ associated with the maximum value of the P_2 parameter. The main difference in the shapes of theoretical lines is the small loop present in the case of CCC predictions but is absent in RDWA data. A similar little structure is also noticeable in experimental results, but in that case the loop is placed closer to the center of the coordinate system.

V. CONCLUSIONS

Our experimental values of the Stokes and EICP parameters are generally in a good agreement with CCC theoretical results. The SC RDWA and MC RDWA data are consistent with presented CCC results for larger scattering angles. In the range 10° to 40° the MC RDWA model predicts most of the characteristic features visible in the graphs of the presented parameters, but with much smaller amplitudes. However, such effects are not reproduced in the case of the SC RDWA results. The observed differences of the experimental, CCC, and RDWA both P_L and γ parameters at scattering angles below 40° indicate a need of improving theoretical models. Therefore, present data are a stimulus for further experimental and theoretical research on the excitation of zinc atoms at lower electron energies, which can help to explain the present discrepancies and result in improvement of theoretical models.

ACKNOWLEDGMENTS

We are grateful to Tapasi Das and Prof. Rajesh Srivastava for providing their theoretical RDWA results in numerical form. This work was supported by Curtin University and the Pawsey Supercomputing Centre.

[1] J. Franck and G. Hertz, Verh. Dtsch. Phys. Ges. **16**, 457 (1914).
[2] B. Bederson, Comments At. Mol. Phys. **1**, 65 (1969).
[3] M. Eminyan, K. B. MacAdam, J. Slevin, and H. Kleinpoppen, Phys. Rev. Lett. **31**, 576 (1973),
[4] N. Andersen, J. W. Gallagher, and I. V. Hertel, Phys. Rep. **165**, 1 (1988).
[5] J. Goeke, G. F. Hanne, and J. Kessler, J. Phys. B **22**, 1075 (1989).
[6] T. Simon, M. Sohn, G. Hanne, and K. Bartschat, J. Phys. B **23**, L259 (1990).
[7] M. Sohn and G. Hanne, J. Phys. B **25**, 4627 (1992).
[8] H. Hamdy, H. J. Beyer, and H. Kleinpoppen, J. Phys. B **26**, 4237 (1993).
[9] H. J. Beyer, H. Hamdy, E. I. M. Zohny, K. R. Mahmoud, M. A. K. El-Fayoumi, H. Kleinpoppen, J. Abdallah, Jr., R. E. H. Clark, and G. Csanak, Z. Phys. D **30**, 91 (1994).
[10] C. J. Bostock, D. V. Fursa, and I. Bray, Phys. Rev. A **82**, 022713 (2010).
[11] C. J. Bostock, D. V. Fursa, and I. Bray, Phys. Rev. A **85**, 062707 (2012).
[12] T. Das, L. Sharma, R. Srivastava, and A. D. Stauffer, Phys. Lett. A **378**, 641 (2014).
[13] L. Pravica, J. F. Williams, D. Cvejanovic, S. Samarin, K. Bartschat, O. Zatsarinny, A. D. Stauffer, and R. Srivastava, Phys. Rev. A **83**, 040701 (2011).
[14] J. F. Williams, L. Pravica, and S. N. Samarin, Phys. Rev. A **85**, 022701 (2012).
[15] K. Bartschat and O. Zatsarinny, Phys. Rev. A **87**, 016702 (2013).
[16] C. J. Bostock, D. V. Fursa, and I. Bray, Phys. Rev. A **87**, 016701 (2013).
[17] M. Born, J. Phys. D: Appl. Phys. **34**, 909 (2001).
[18] M. Piwiński, Ł. Kłosowski, D. Dziczek, S. Chwirot, T. Das, R. Srivastava, A. D. Stauffer, C. J. Bostock, D. V. Fursa, and I. Bray, Phys. Rev. A **86**, 052706 (2012).
[19] M. Piwiński, D. Dziczek, Ł. Kłosowski, and S. Chwirot, Eur. Phys. J. S. T. **222**, 2273 (2013).
[20] Ł. Kłosowski, M. Piwiński, D. Dziczek, K. Wiśniewska, and S. Chwirot, Meas. Sci. Technol. **18**, 3801 (2007).
[21] I. V. Hertel and W. Stoll, J. Phys. B **7**, 570 (1974).
[22] J. Macek and I. V. Hertel, J. Phys. B **7**, 2173 (1974).
[23] D. Dyl, D. Dziczek, M. Piwiński, M. Grądziel, R. Srivastava, R. Dygdała, and S. Chwirot, J. Phys. B **32**, 837 (1999).
[24] D. Dziczek, D. Dyl, M. Piwiński, and S. Chwirot, Acta Phys. Pol. A **93**, 717 (1998).
[25] M. Piwiński, D. Dziczek, R. Srivastava, M. Grądziel, and S. Chwirot, J. Phys. B **35**, 3821 (2002).
[26] D. Dziczek, M. Piwiński, M. Gradziel, and S. Chwirot, Acta Phys. Pol. A **103**, 3 (2003).
[27] M. Piwiński, D. Dziczek, Ł. Kłosowski, R. Srivastava, and S. Chwirot, J. Phys. B **39**, 1945 (2006).
[28] Ł. Kłosowski, M. Piwiński, D. Dziczek, K. Pleskacz, and S. Chwirot, Phys. Rev. A **80**, 062709 (2009),
[29] S. A. Napier, D. Cvejanović, J. F. Williams, L. Pravica, D. Fursa, I. Bray, O. Zatsarinny, and K. Bartschat, Phys. Rev. A **79**, 042702 (2009).
[30] D. V. Fursa and I. Bray, J. Phys. B **30**, 757 (1997).
[31] D. V. Fursa and I. Bray, Phys. Rev. Lett. **100**, 113201 (2008).
[32] I. C. Percival and M. J. Seaton, Phil. Trans. R. Soc. A **251**, 113 (1958).